CrossMark

ORIGINAL ARTICLE

Hunza river watershed landslide and related features inventory mapping

M. Farooq Ahmed[1] · J. David Rogers[2] · Muhammad Zubair Abu Bakar[3]

Abstract This study summarizes the continuation of a series of regional landslide inventories undertaken in Northern Pakistan. Mass wasting appears to be the dominant process shaping the morphology of the main river channel in the Hunza River watershed. The project included assembling an inventory of historic mass wasting features in the basin, especially, those along the Hunza River. A hillshade topographic map was created by stitching ASTER Digital Elevation Models (DEMs) with 30 m resolution topographic sheets of 40 m resolution, using ArcGIS. The methodology utilizes anomalous topographic expression (i.e., parallel and converging drainage patterns, divergent contours, crenulated contours, and isolated knobs) to identify landslide features. The screening process includes examination of topographic anomalies and inconsistencies, which are typical of landslides and related mass wasting features. The mapped landslide features included a number of historic landslides in the area. Historic landslide damming of the Hunza River has occurred at Attabad, Boultar Glacier, Gannish-Chiss, and Ganesh-Saukien. The outbreak floods associated with the overtopping of these recent landslide dams often leave anomalous geomorphic signatures, which were identified in the terrain analysis, and helped validate the interpretations made as part of this study. Such products serve as guide maps for more detailed analyses of specific sites, as might be under consideration for structures, highways, tunnels, dams, powerhouses, or utility corridors.

Keywords Hunza River · Landslide · Inventory mapping · Lithology · Hillshade maps

Introduction

Landslides can occur in almost any landform; provided that the conditions exist that are adverse to long-term stability. The destabilizing factors vary from one site to another, but appear to be influenced by the underlying geologic structure, steepness of slope, slope height and length, moisture content, vegetative cover, and anthropogenic disturbance. The uses of geomorphic and topographic anomalies greatly aid the preparation of landslide inventory maps of any particular area (Hutchinson 1968; Varnes 1978; Hansen 1984; Cruden and Varnes 1996; Ahmed and Rogers 2014, 2015). Various types of slides typically exhibit anomalous topographic expression, related to slope movement, failure extent, depth, and size. These features can be characterized and mapped on aerial photographs, and/or hillshade topographic maps (Varnes 1978; McCalpin 1984; Rogers 1994; Cruden and Varnes 1996). The visual inspection of hillshade maps often reveals topographic anomalous topographic features typical of landslide-prone slopes.

✉ M. Farooq Ahmed
mfanr5@mst.edu

J. David Rogers
rogersda@mst.edu

Muhammad Zubair Abu Bakar
mzubairab1977@gmail.com

[1] Department of Geosciences and Geological and Petroleum Engineering, Missouri University of Science & Technology (On leave from University of Engineering and Technology Lahore, Pakistan), Rolla, MO, USA

[2] Department of Geosciences and Geological and Petroleum Engineering, Missouri University of Science & Technology, Rolla, MO, USA

[3] Department of Geological Engineering, University of Engineering and Technology, Lahore, Pakistan

🙋 Springer

Satellite imagery and shaded digital elevation models of varying resolution are increasingly available, world-wide. These can serve as useful tools in discerning the presence of past landslippage, especially if those features are of sufficient scale to perturb at least five consecutive contours (Ahmed and Rogers 2014). An interpreter should possess sufficient knowledge and experience about the bedrock geology, underlying structure, and the style and mechanisms of mass wasting that characterize the study area.

Evaluations of hill slope profiles are of particular utility in assessing past landslippage (Rogers 1994). Hillslope morphology is largely influenced by geologic settings, localized down cutting of channels due to changes in erosive base level, and climatic changes (Crozier 1973; Selby 1993). A key factor in exploiting topographic information is the density and quality of the data. In general, the more precise mapping results can be obtained for larger maps, where small slides may be delineated with certain degree of precision. The regional level landslide inventories (scales ~1:100,000) can be prepared using aerial photographs and hillshade topographic maps (Cardinali et al. 1990; Brabb 1991; Rogers 1994; Guzzetti et al. 2006; Ahmed and Rogers 2014, 2015).

Mass wasting appears to be the dominant process shaping the morphology of the main river channel in the Hunza River watershed. In most instances, the landslides appear to recur at the same sites over and over, as the debris is removed by successive outbreak floods, on each occasion adding another "generation" of oversized "skeletal blocks." After the first slope failure occurs, usually along pre-existing discontinuities, there exists an unsupported slope in the headscarp evacuation scar. The accumulated debris at the toe of the slide is then subject to rapid excavation and removal by the river. Subsequent slope failures and partial reactivations may ensue, depending on how much debris is dispersed or removed by the river (Lee and Duncan 1975). At the locations of historic landslide dams that have breached (i.e., Attabad, Barut and Ginnesh Saukein events, etc.), the river is still trying to regain its original base level by down-cutting through the slide debris. This situation could be observed in the entire Hunza River basin, where the river appears to flow on a thick sequence of alluvial detritus, and most of the channel terraces have been stabilized by vegetation and support argillic B soil horizons. These features suggest considerable periods of subaerial exposure, especially, in the center of the river valley. All of these events have carbonate source rocks and carbonate cement similar to breccias. Dozens of villages are situated on old rock avalanche debris, including Gupis, Sost, and Karimabad-Ganesh.

The current study utilized anomalous topographic protocols (i.e., parallel and converging drainage patterns, divergent contours, crenulated contours, isolated knobs, etc.) to delineate and map various type landslides related features in the Hunza River Basin. The resultant inventory map was further compared and validated with the available historic records of landslides in the basin (Hewitt 2002; Korup et al. 2010; Hewitt et al. 2011).

Study area

The Hunza River originates at the confluence of the glacially-fed Kilik and Khunjerab Nalas (Fig. 1), which is joined by the Gilgit and Naltar Rivers before emptying into the Indus River. This is one of the principal rivers of Gilgit–Baltistan, Pakistan. The Hunza River encompasses a drainage area of 8000 km^2 and flows northwest to southeast, cutting through the Karakoram Range. The watershed contains numerous peaks rising to more than 6000 m elevation, including many snow covered peaks, like Rakaposhi (7788 m), Ultar Sar (7388 m), Ghenta Peak (7090 m), and Hunza Peak (6270 m). The upper reaches of the Hunza River freeze in the winter, and the narrow channel constricts the flows within the river valleys. As the snow melts in the higher elevations during the summer, the river's flow swells noticeably, often overflowing its banks and inundating the adjacent areas, up to several kilometers.

The severe climate variance between the highlands and the semi-arid valleys also leads to significant erosion and mechanical weathering of the rocks. The river valleys have a thick cover of quaternary and recently deposited sediments containing glacial, debris flow, rock avalanche debris, and lacustrine deposits (Owen 1991).

Northern Pakistan straddles three different tectonic provinces: the Indian Plate in the south extends from the Nanga Parbat to the Peshawar Basin; the Kohistan-Ladakh magmatic arc occupies the central part; and the Karakoram Plate underlies the most northern sub-region (Kazmi and Jan 1997). The region is known for high rates of tectonic uplift and seismicity (Shehzad et al. 2009; Korup et al. 2010).

The geologic formations exposed in the study area are shown in Fig. 2. These include: the Karakoram batholith and associated plutons (Tkk) of Miocene to Cretaceous age, the Kohistan-Ladakh batholith and associated plutons (Tkb) of Miocene to Cretaceous age, the Kilik (CDK) and Baltoro (Cb) formations of the northern Karakoram Range, of Carboniferous to Devonian age, and the Shaksgam and Gircha formations (Ps–Pg) comprising the Hindukush-Karakoram Belt of Permian age. The Chalt Volcanics and Yasin group undivided (KJcy) are of Cretaceous to Jurassic age. Mesozoic to Paleozoic Rocks (MPzs) include metasedimetary rocks of the Eastern Kohistan Arc, Jurassic to Paleozoic age metamorphic

Fig. 1 Generalized map of the Hunza River watershed, and location of the study area (at *upper right*)
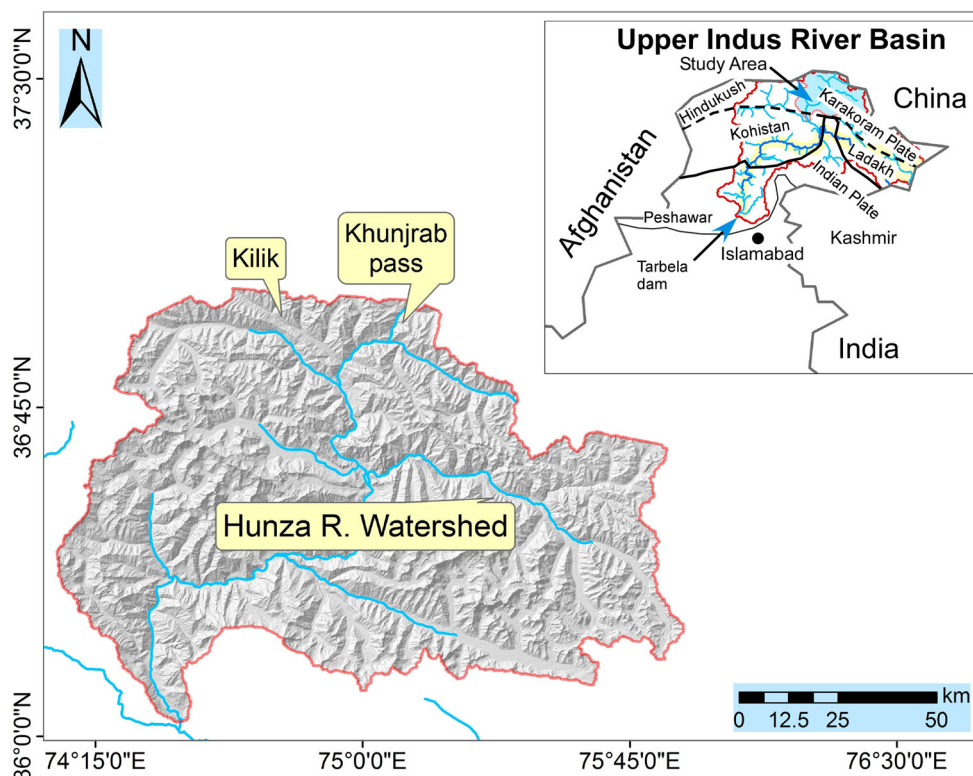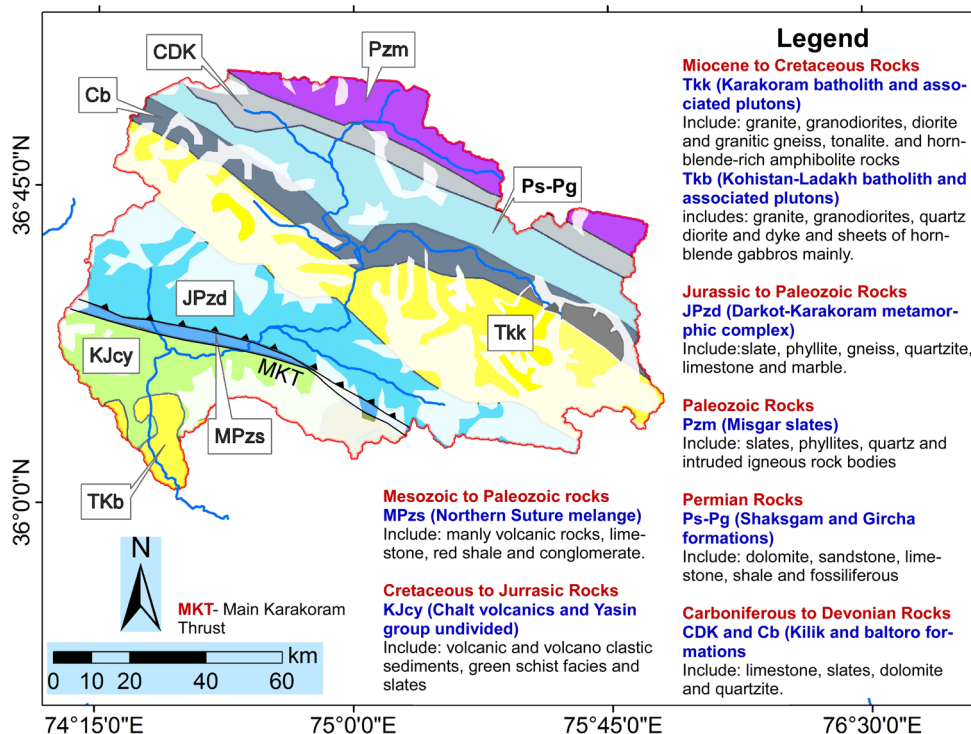

Fig. 2 Digitized geology map of the Hunza River Watershed (data from Geological Map of Pakistan 1993)

complex (JPzd) of the Hindu Kush-Karakoram, and the Darkot-Karakoram metamorphic complex (JPzd) of Jurassic to Paleozoic age. Brief descriptions of these units are provided on Fig. 2. Active faults, like the Main Karakoram Thrust (MKT), and weaker units, such as shales, slates, and phyllites, make this region more susceptible to mass wasting phenomenon, which is evident from the number of documented slides in the area.

Slope profiles are noticeably perturbed by past lands-liding and appear to be structurally controlled. Translational block slides and rock avalanches appear to be the predominant physical process shaping the slopes of the Hunza River watershed (Hewitt 1982). Most of the upper slopes lie above 5000 m and are snow covered, making glacial avalanches a common occurrence during certain times of the year. The lower slopes are typified by deep incision of the Hunza River, suggestive of the rapid down cutting. It is along these over-steepened slopes that a large number of massive bedrock landslides have dumped into the river valleys. The age of the largest slides appears to be late Pleistocene, or >11 ka. However, the surfaces of the old landslides are actively eroding and criss-crossed by younger and relatively smaller individual slides, which are much easier to discern.

Methodology

The hillshade topographic map was created in ArcGIS by stitching the ASTER Digital Elevation Models (DEMs) with 30 m resolution, downloaded from ASTER GDEM website (http://www.jspacesystems.or.jp/ersdac/GDEM/E/index.html), and 1:200,000 topographic sheets with 40 m elevation contours, obtained from an online source 'Topographic Maps of the World' (www.mapstor.com). The data resolution is adequate to delineate landslide features >500 m high/long). To delineate noticeable changes in surface topography indicative of mass wasting, a minimum of five consecutive contour intervals length along the slope is required (Ahmed and Rogers 2014). For this inventory mapping, a 40 m contour topographic map would only be able to discern landslide features perturbing at least five adjacent contours (40 × 5 = 200 m vertical relief). For slopes of ∼2:1 (horizontal to vertical) inclination, the smallest landslide feature would have to be at least ∼500 m on horizontal scale, against the elevation difference of ∼250 m (Ahmed and Rogers 2014, 2015).

Hillshade topographic mapping sheets of the study area were printed on sheets measuring approximately 122 × 92 cm using ArcGIS 10 to visually delineate land-slide features using a pencil. The identified landslides features were then digitized and geo-referenced with the original hillshade map in ArcGIS. Anomalous geomorphic signatures are usually indicative of various type of mass wasting processes (Crozier 1973; Rogers 1980, 1994; Cruden and Varnes 1996; Crosta 2001; Doyle and Rogers 2005). These anomalous features were utilized to prepare the regional landslide inventory of the study area.

The physical manifestations of anomalous key indicators generally vary according to the different stages of the erosion cycle dominating a particular area or region. The most recent slides usually exhibit sharp and definite boundaries, but older slides are increasingly difficult to discern precisely (Angeli et al. 1996). Various types of slides were recognized and classified by their respective topographic expression. The most common expressions were: (1) *divergent contours* that curve upslope and downslope, suggestive of the deflation in the upper part and inflation in the lower part of the slide; (2) *isolated topographic* benches are flat areas below the headscarp formed by back-rotation of slumped masses; (3) *isolated topographic knobs* formed by deep-seated translational bedrock slide movement cause separation of a ridge's caprock; (4) *crenulated contours show waviness in their shape,* often key indicator for an out of equilibrium slide and diagnostic of flow slides and rock avalanches. A few examples of these anomalous topographic signatures are briefly described below.

Rotational and retrogressive slumps

The geometry of rotational slumps depends on the thickness and consistency of the weathered rock mass being affected (Fig. 3a). Thick zones of soil, colluvium, and detritus from bedrock creep zones often foster simple, spoon-shaped slumps (Varnes 1958). A classic feature of rotational slumps within bedrock units is the topographic expression of back-rotated grabens, which form isolated topographic benches (Fig. 3a).

Retrogressive rotational slumps are a common failure mode within weathered shales (Zaruba and Mencl 1982). Previous retrogressive slumping usually forms multiple isolated topographic benches and in plan, these features often appear as a series of small terrasets (Sharpe 1938).

Debris flow

Past debris flow activity can often be discerned by noting opposing contours in the basins situated in the steep-sided slopes. Figure 3b shows inward-shaped contours opposed by outward-shaped contours, which are usually indicative of recent flow slides. Coalescing debris lobes usually form where the lower slopes diminishes in slope, most commonly, at grades less than 12 % slope (and up to 50 %, depending on the coarseness and angularity of the debris). These flow lobs can cause constrictions of bedrock channels that can be preserved for hundreds of years (Rodine 1974; Reneau 1988). Debris fans appear topographically similar to alluvial fans; but are typically much steeper (alluviation usually occurring on gradients of 1.5 % or less).

Fig. 3 Anomalous topographic expressions characteristic of various types of landslides; **a** planar rotational slump, **b** Combination Earth/debris flow 10–100 years old on *left*, and 100–500 years old on *right*, **c**, **d** typical earthflow/slump complex (Rogers 1994)
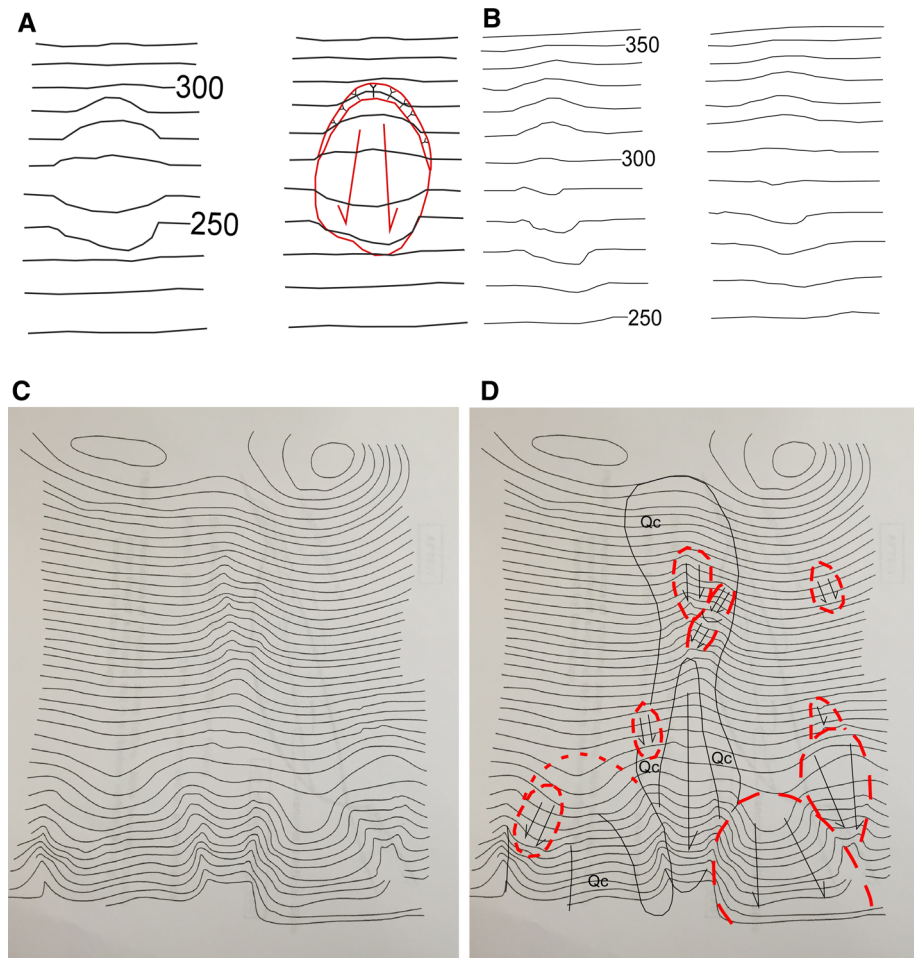
Earthflows

Earthflows are easily identified by their distinctive divergent contours within the hillslopes as they tend to spawn broad, circular-shaped headscarp evacuation areas (Keefer and Johnson 1983; Varnes 1978; Fig. 3c, d). The older earthflow slides could be recognized by crenulated flow lobe contours that are laterally restricted (Ibsen et al. 1996).

Translational bedrock slides

Translational landslides/block glides are those which moved as a semi-coherent block upon a discrete failure surface (non-circular), usually along pre-existing geologic discontinuities (Miller 1931; Varnes 1958; Rogers 1998). Translational slides tend to be larger features, generally involving weathered bedrock, which usually possesses greater shear strength that soil or colluvium slides. Dormant bedrock slides are often overlooked by geotechnical practitioners if the boundaries are smoothed over and mollified. One of the best indicators of prehistoric bedrock sliding is perturbed first-order drainages, especially parallel gullies that terminate well short of a drainage divide, anomalous pear-shaped masses between well-developed ridges, anomalous topographic benches, and isolated knobs. Figure 4 shows the most common topographic expressions of translational bedrock failures.

Complex and composite landslides

Complex slides are those that commonly exhibit at least two types of movement in sequences, such as translational sliding, followed by spreading and flowing. Composite landslides exhibit two or more types of movement simultaneously, in different parts of the sliding mass. This would include back-rotational grabens forming above translational slides, shown in Fig. 5. Some of the lesser-appreciated failure modes common to the area include toppling (Fig. 6), which may precede rock avalanches triggered by seismic shaking. Shallow slumps and flow slides often mantle deeper-seated translational slides, as sketched in Fig. 7. All of the slides mapped in this study are deep-seated, which connotes failure surfaces that extend into the underlying bedrock units, and not necessarily confined to
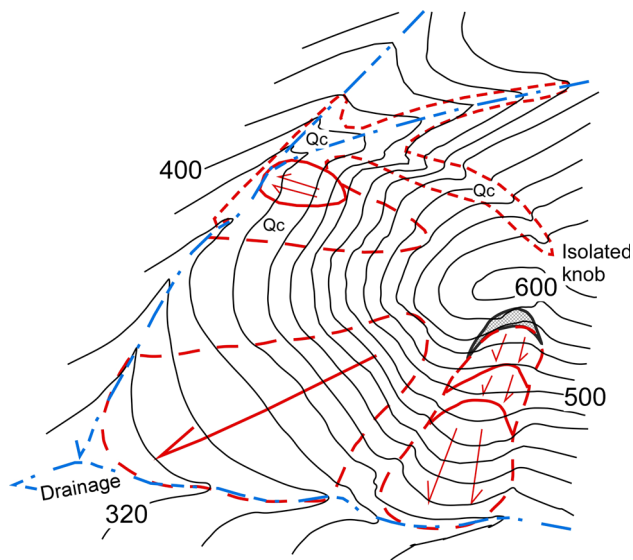
Fig. 4 Topographic expressions of dormant translational and smaller, secondary slides, often triggered by toe erosion and displacement of adjacent blocks

the soil regolith. Most of the slides we identified could be classed as complex, compound, translational, retrogressive, slump-flows, topples, or rock avalanches.

Results and discussion

The landslide inventory mapping includes all manner of bedrock landslides, some of which may be as old as the Pleistocene-Holocene transition, 11,000 y.b.p. The landslide inventory is simply a fair approximation of the most topographically prominent landslides, measuring more than 500 m long (Fig. 8). Data gleaned from the landslide hazard maps of the Indus River Basin (Ahmed and Rogers 2012, 2014, 2015; Ahmed et al. 2014) and documented rockslides (Hewitt 1982, 2002; Shroder 1998; Shroder and Bishop 1998; Korup et al. 2010; Hewitt et al. 2011) were utilized for the validation of our interpretations. The comparison exhibits a satisfactory match of the landslide features mapped with those reported across the study area.
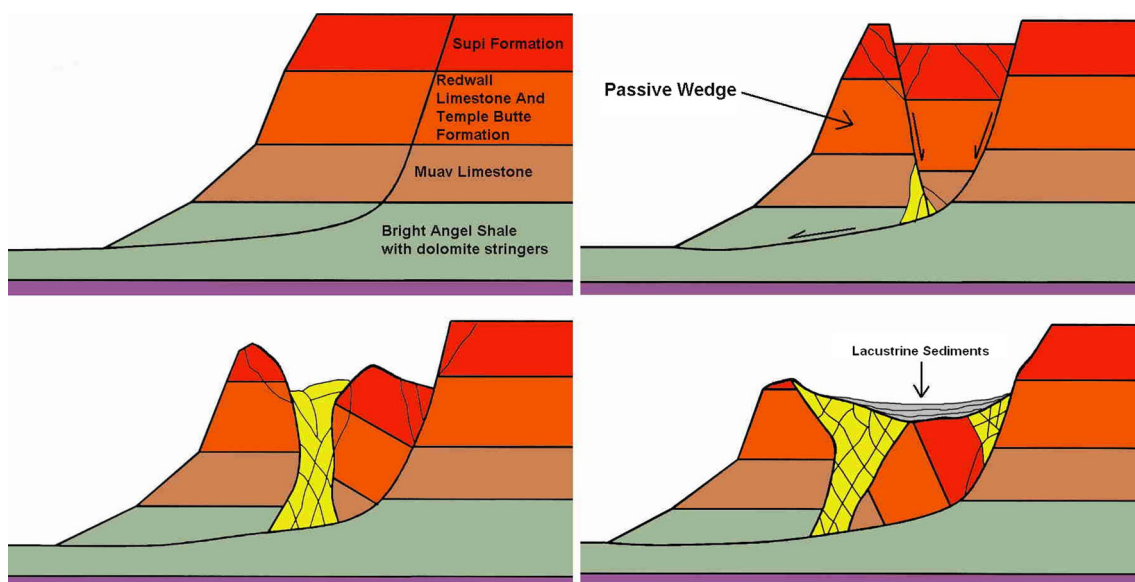

Fig. 5 Example of a composite landslide, where translation and back-rotation and brecciation (indicated by cross-hatching) occur simultaneously. This is the Thunder River Landslide in the Grand Canyon (Watkins et al. 2007)

Fig. 6 Flexural toppling initiates along steeply-inclined discontinuities, like foliation, as shown at *left*. As the individual blocks continue toppling, a planar detachment surface develops, as seen at *right*. The displaced mass can then be loosened as a rock avalanche during severe earthquake shaking
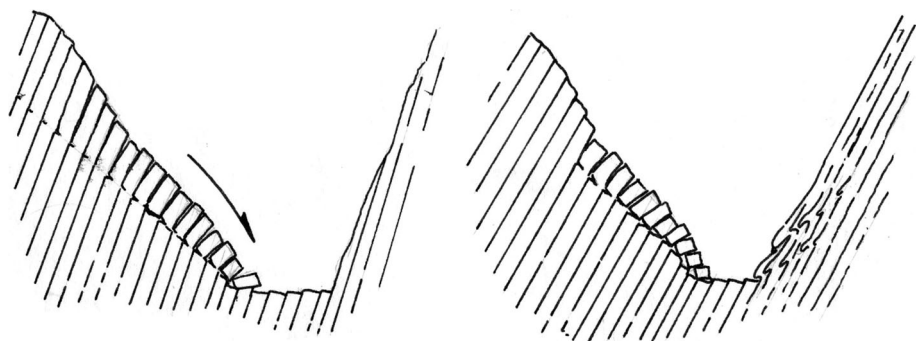
A few of those events, along with their probable mapped traces (using anomalous topographic expressions) are described below.

The Shikar Jerab, Bordon Tir-Sost and Barut Hunza (SJ, BT-S and BH events, respectively on Fig. 8) are significant

pre-historic rock avalanche events that occurred along the Hunza River. Figure 9a presents an excerpt of the landslide inventory map in the vicinity of these events in the Hunza Valley. The topographic expressions of SJ are typical of healed earth flow/retrogressive rotational slump those can

Fig. 7 Block diagram illustrating colluvial infilling and small *scale* mass wasting that often develops upon deep-seated translational or rotational block slides (from Rogers 1994)
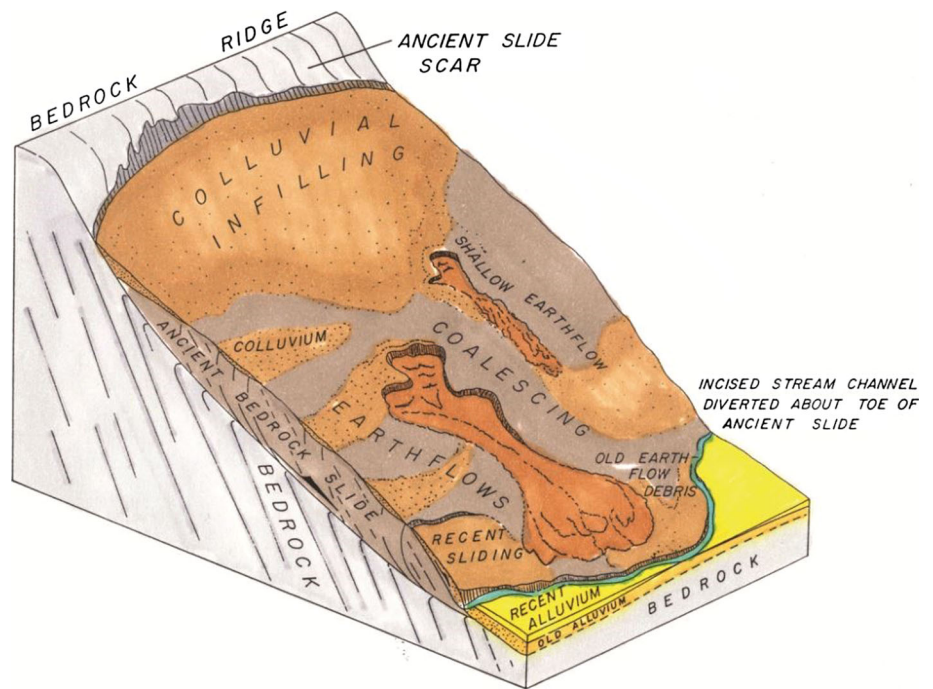
Fig. 8 Landslide inventory map (*yellow*) with documented historic slides shown as *red dots*

BT-S: Bordon Tir-Sost
SJ: Shikar Jerab
BH: Barut Hunza
AT: Attabad dam
GS: Gannish-Saukien
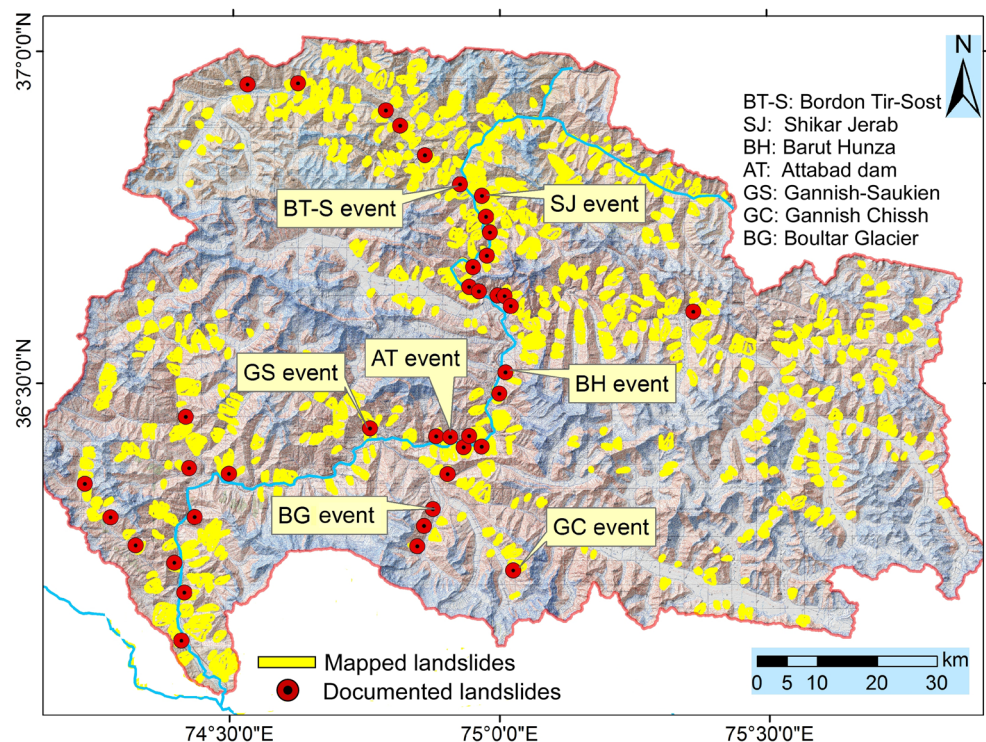GC: Gannish Chissh
BG: Boultar Glacier

Fig. 9 **a** Excerpt of landslide inventory map in vicinity of the historic Shikar Jerab landslide dam, along the Hunza River near Sost, **b** cross-section of the Shikar Jerab landslide, with inferred slide depths and volumes, based on the valley profiles. This profile illustrates the likely impact of multiple events at this location, which likely spawned outbreak floods in several stages. The dashed red lines show the inferred pre-slide topography and oldest/deepest incision of the channel at this location
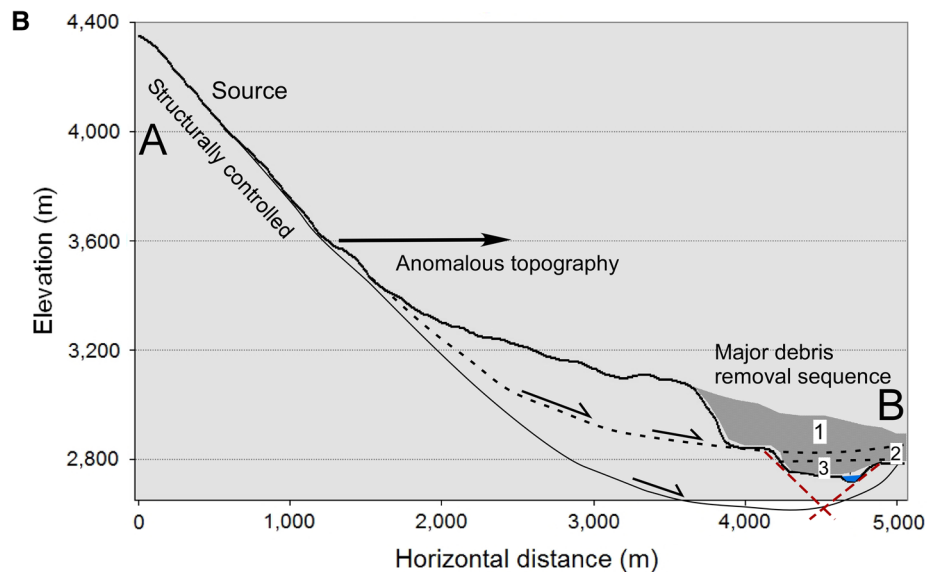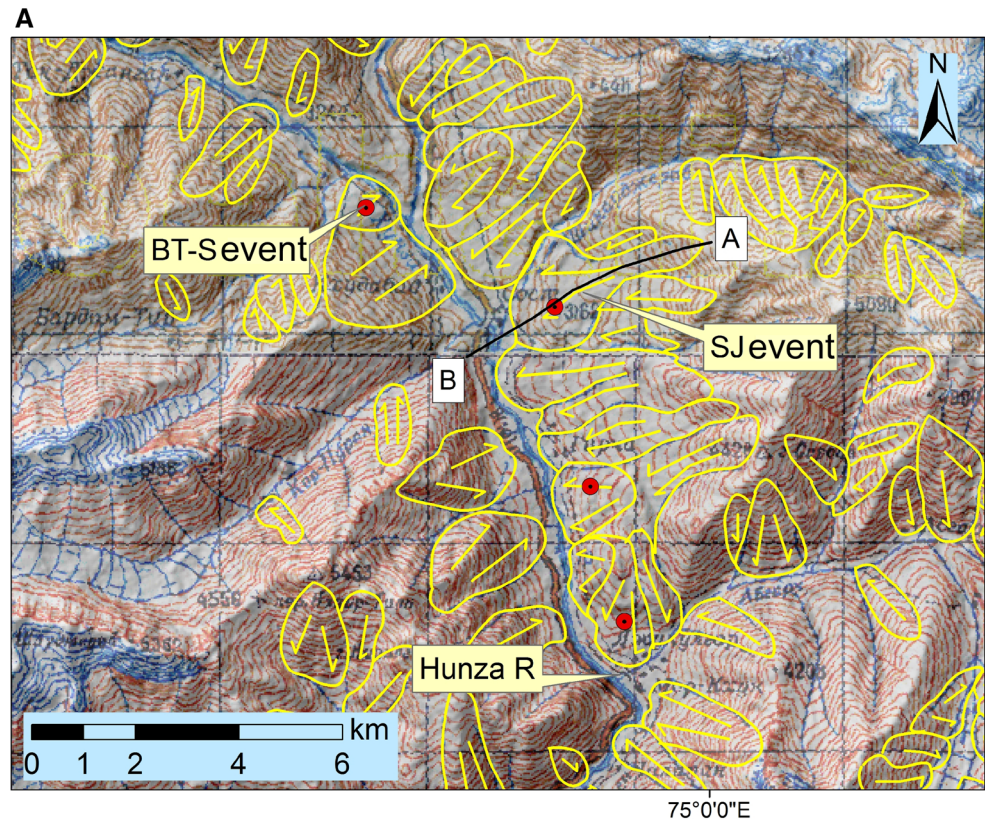
be identified by their distinctive divergent contours and by crenulated flow lobe contours that are laterally restricted within the hillslopes (see also Fig. 3c, d)." The BT-S prehistoric landslide event is likely a translational bedrock failure or planner bedrock slumps that has an anomalous pear-shaped mass a well-developed ridge, and isolated knobs (see also Fig. 4).

The rock avalanches were comprised of cemented carbonate debris, which is well preserved at their respective locations (Hewitt 2002). The profile of Shikar Jerab rock avalanche shows a sufficient volume of debris carried into the channel, and the river's flow was likely halted until it began to overflow the debris dam, along the opposing channel bank. The water stored behind the debris dam helped the rapid excavation of a new channel, cutting downward from the point of initial overtopping, on the opposite channel bank.

The most recent landslide dam in the study area formed on 4 January 2010 near Attabad village (AT event on

Fig. 10 Google Earth view of the 2010 Attabad landslide dam, showing the probable extent of the failure. The *smaller* image shows the tension cracks exposed in the village of Attabad, a few years before the event
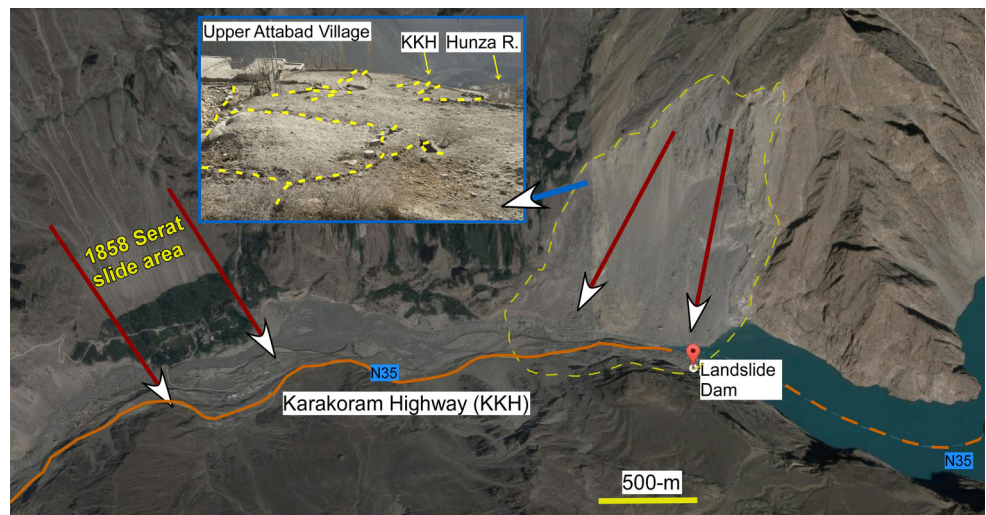

Fig. 8). The debris dam is 120 m high and impounded a reservoir 21 km long. The landslide was triggered by the movement of an active fault, aided by a pre-existing compound slide with known stability issues (Fig. 10). A part of Attabad village was situated on the middle left side of the dormant bedrock slide. Prior to the 2010 failure, several tension cracks were noticed in the upper Attabad Village over a period of several years. The slide mass has an estimated volume of 30 million m^3. It cascaded down from the northern valley wall, falling onto saturated lake sediments (lacustrine deposits), deposited behind the 1858 Serat landslide dam at Salmanabad, a few kilometers downstream (Fig. 10). The Serat rock avalanche blocked the Hunza River for more than 7 months, and subsequently triggered then second largest flood event in the norther Pakistan (the Lichar Gah outburst flood of 1842 along the Indus River was larger; Becher 1859; Todd 1930).

The lowest saddle of the Attabad debris dam rises 140 m above the river, filling the channel for a distance of over a kilometer. The main portion of the landslide dam is comprised of colluvial material in a fine, sandy matrix, with isolated blocks of granite and granodiorite. The clasts are generally angular, ranging in size from a few centimeters to >10 m. This landslide dam poses a significant threat to the neighboring villages, as well as the inhabitants downstream, all the way to Tarbela Reservoir.

The pre-failure topographic signatures at Attabad are shown on the hillshade map (Fig. 11a). The well-developed ridges, anomalous topographic benches, and isolated knobs are common topographic expressions of translational bedrock slides. The profile on the left side of Fig. 11b shows the pre-failure condition, which the authors interpreted to be a dormant bedrock slide. The grey shaded area is a headscarp evacuation graben, which often infill with loose colluvial debris that allows infiltration of precipitation and tributary runoff.

Ganesh-Saukien is another example of a pre-historic rock avalanche (GS event on Fig. 8). This rock avalanche remnants was traced out on the inventory map by observing the anomalous topography (comparing topographic profiles with the surrounding hillslopes). The topographic expressions of this slide are typical of a healed earth flow/retrogressive rotational slump. Substantive deposits of rock avalanche debris slides at the junction of three populated valleys. The successive rock avalanches in this vicinity are likely associated with assemblages of intensively crushed and complexly sheared blocks, with distinctive lithologies that Hewitt (2002) was able to discern from less disturbed outcrops in the near vicinity.

The Pre-historic Gannish Chissh rock avalanche (GC event on Fig. 8) detached from a summit elevation over 7000 and fell 2000 m, onto the upper Barpu Glacier, and later transported down the valley, leaving significant remnant deposits along the river channel. The topographic expression of this event was not easily discernable because of subsequent glacial retreat, but the field observations by Hewitt (2002) have documented the event.

The 1986 Boultar Glacier event was the first rock avalanche reported in Karakorum, within the Hunza River watershed (Hewitt 1998, BG event on Fig. 8). The avalanche dropped 1400 m and its debris field covered an area of 3.5 km^2. The rock avalanche was first to befall the Boultar Glacier in historic time. The debris was reworked by the glacial ice for a few years before being transported approximately 4 km by the glacier, down to the river valley (Gardner and Hewitt 1991). Hewitt 2002 observed the open work surface of the rock avalanche debris field, which included mega-clasts, composed of broken and crushed marble and large boulders. There are more rock avalanches in this region, most of which originate from over-steepened canyon walls rising 4500 m above the channels. Several of these subsequently fell on the Boultar Glacier before being transported into the valleys (Hewitt 2002).
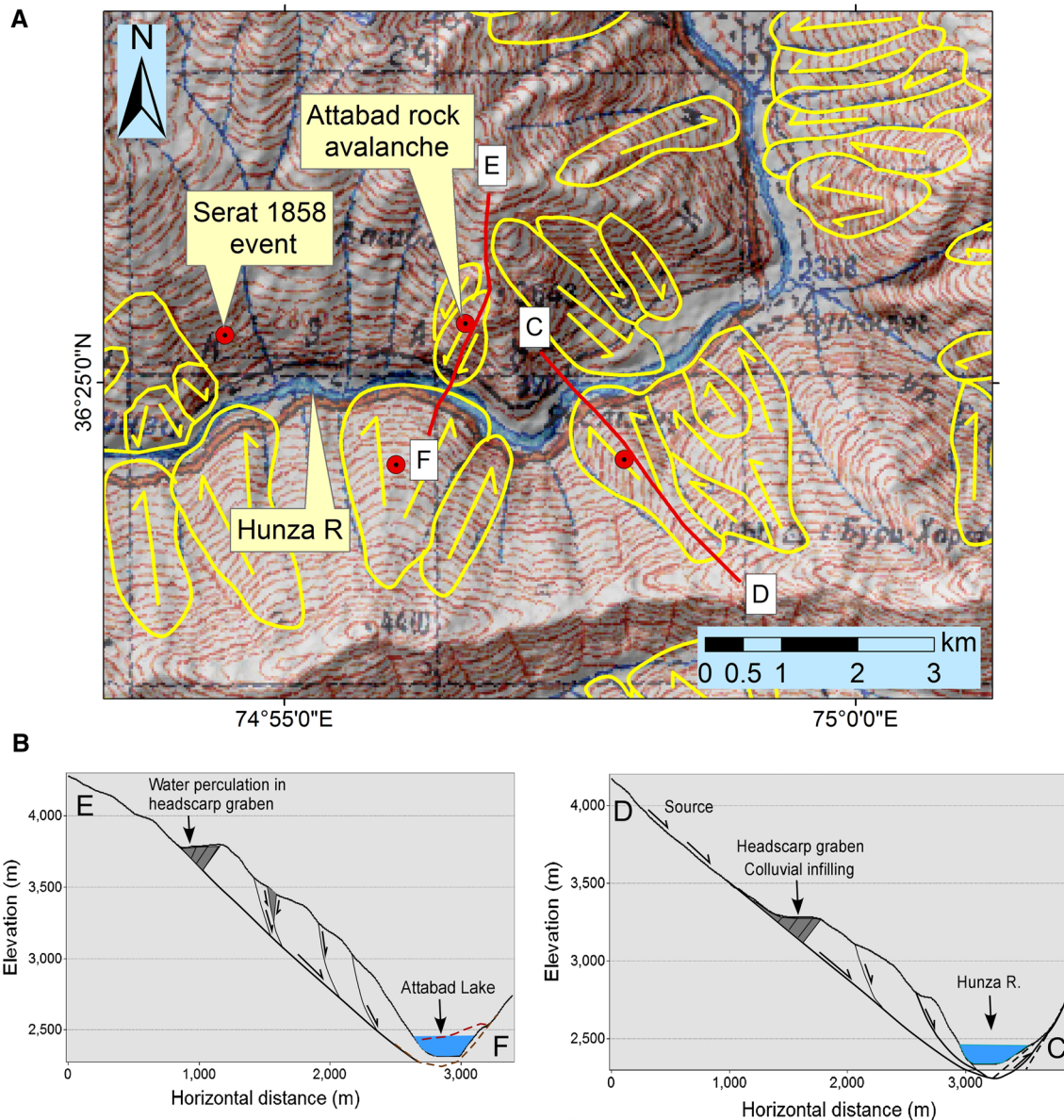
Fig. 11 a Excerpt of landslide inventory map showing the location of the 2010 Attabad landslide dam and other landslides in the vicinity, b section *E–F* at left shows the pre-failure surface of the Attabad rock avalanche. Section *D–C* illustrates a similar type of slide, a few kilometers upstream of the Attabad slide. Both of these profiles are typical of planar translational bedrock slides, structurally controlled by discontinuities, with headscarp regression and infilling of head-scarp grabens with colluvium

Reconnaissance-level mapping of landslide features on topographic maps involves considerable 'expert knowl-edge' and discretion to delineate the areal extents of slide features because of the resolution of the available data and colluvial infilling and secondary mass wasting, which tends to mollify those boundaries (as illustrated in Fig. 7). For these reasons, a certain degree of error should be expected, even under the best conditions. An interpreter should possess adequate knowledge and understanding about the bedrock geology, underlying structure, and the mechanisms of mass wasting that characterize the study area.

The current study has successfully utilized anomalous topographic protocols to delineate and map various types of landslides related features in the Hunza River Basin. The resultant inventory map was then compared with available historic records of landslides in the basin, to validate the methods undertaken. This study reveals that the mass wasting appears to be the dominant process shaping the morphology of the Hunza River watershed. Subsequent slope failures and partial reactivations of older slides at the locations of historic landslide dams along the principal water courses suggest that these channels are still trying to

regain their original base level by excavating their beds in the slide debris. These former landslide dam sites form discernable knickpoints in the channels because of thick sequences of alluvial detritus.

Conclusions

This project began as a concerted effort to explore low-cost indirect methods to validate regional inventory mapping of landslide-related features. The study suggests that the Hunza River watershed supports a significant number of recent and ancient bedrock landslides, based on the historic records and anomalous topographic features. The sequence of events observed repeatedly at dozens of locations suggests that large rock slope failures noticeably impact the river's longitudinal profile. This take-away is significant and worthy of more attention in fluvial geomorphology. The most common types of slides included complex, compound, translational, retrogressive, slump-flows, topples, and rock avalanches. These deep seated slides are more common along the lower slopes, within the over steepened slopes of incised bedrock channels. The interpretations of slope profiles through rock avalanche sites consistently exhibit knickpoint and rapids, attesting to repeated episodes of stream channel entrenchment, infilling, and retrenchment. This reconnaissance level inventory that was intended to serve as a guide for where more detailed investigation of some potential sites of interest might be undertaken, such as infrastructure projects in the region.

Acknowledgements

References

Ahmed MF, Rogers JD (2012) Landslide Mapping and Identification of old Landslide dams along the Indus River in Pakistan, using GIS Techniques. AEG 55th Annual Meeting, Salt Lake City, Utah 55:44

Ahmed MF, Rogers JD (2014) Creating reliable, first-approximation landslide inventory maps, using ASTER DEM data and geomorphic indicators, an example from the upper Indus River in northern Pakistan. Environ Eng Geosci 20(1):67–83

Ahmed MF, Rogers JD (2015) Regional level landslide inventory maps of the Shyok River watershed, Northern Pakistan. Bull Eng Geol Environ. doi:10.1007/s10064-015-0773-2

Ahmed MF, Rogers JD, Ismail EH (2014) A regional level preliminary landslide hazard study of upper Indus River basin. Eur J Remote Sens 47:343–373

Angeli MG, Gasparetto P, Menotyti RM, Pasuto A, Silvano S, Soldati M (1996) Rock avalanche, Art. 8.2. In: Dikau R, Brunsden D, Schrott L, Ibsen M-L (eds) Landslide recognition, identification, movement and causes. Wiley, New York, pp 190–201

Becher J (1859) Letter addressed to RH Davis Esq. Secreretary to the Government of the Punjab and its dependencies (on the Indus flood). J Asiat Soc Bengal 28:219–228

Brabb EE (1991) The World landslide problem. Episodes 14(1):52–61

Cardinali M, Guzzetti F, Brabb EE (1990) Preliminary map showing landslide deposits and related features in New Mexico. US Geological Survey Open File Report 90/293, 4 sheets, scale 1:500,000

Crosta GB (2001) Failure and flow development of a complex slide: the 1993 Sesa landslide. Eng Geol 59:173–199

Crozier MJ (1973) Techniques for morphometric analysis of landslips. Zeitschrift fur Geomorphologie 17(1):78–101

Cruden DM, Varnes DJ (1996) Landslide types and processes. In: Turner AK, Schuster RL (eds) Landslides, investigation and mitigation, special report 247. Transportation Research Board, Washington D.C, pp 36–75

Doyle BC, Rogers JD (2005) Seismically-induced lateral spread features in the western New Madrid seismic zone. Environ Eng Geosci 11(3):251–258

Gardner JS, Hewitt K (1991) A surge of the Bultar Glacier, Karakoram range, Pakistan: a possible landslide trigger. J Glaciol 32(112):27–29

Geological Map of Pakistan (1993) Geological Survey of Pakistan Graphic Publishers, Karachi. Scale 1:1,000,000

Guzzetti F, Reichenbach P, Ardizzone F, Cardinali M, Galli M (2006) Estimating the quality of landslide susceptibility models. Geomorphology 81:166–184

Hansen A (1984) Landslide hazard analysis. In: Brunsden D, Prior DB (eds) Slope instability. Wiley, New York, pp 523–602

Hewitt K (1982) Natural dams and outburst floods of the Karakoram Himalaya. In: Glen J (ed) Hydrological aspects of Alpine and high mountain areas., 138International Hydrological Association Publication, UK, pp 259–269

Hewitt K (1998) Catastrophic landslides and their effects on the Upper Indus streams, Karakoram Himalaya, northern Pakistan. Geomorphology 26:47–80

Hewitt K (2002) Styles of rock-avalanche depositional complexes conditioned by very rugged terrain, Karakoram Himalaya Pakistan in Evans, SG, and Degraff, JV, eds, Catastrophic Landslides: Effects, occurrence, and mechanisms. Boulder, Colorado, Geological Society of America, Reviews in Engineering Geology 15: 345–377

Hewitt K, Gosse J, Clague JJ (2011) Rock avalanches and the pace of late Quaternary development of river valleys in the Karakoram Himalaya. Geol Soc Am Bull 123(9/10):1836–1850

Hutchinson JN (1968) Mass Movement. In: Fairbridge RW (ed) The Encyclopedia of Geomorphology. Reinhold Book Corp, New York, pp 688–696

Ibsen ML, Brunsden D, Bromhead E, Collison A (1996) Flow Slide, Art. 8.3. In: Dikau R, Brunsden D, Schrott L, Ibsen M-L (eds) Landslide recognition, identification, movement and causes. Wiley, New York, pp 202–211

Kazmi AH, Jan MQ (1997) Geology and tectonics of Pakistan. Graphic Publishers, Karachi, p 554. ISBN 9698375007

Keefer DL, Johnson AM (1983) Earth flows—morphology, mobilization, and movement. US Geol Surv Prof Pap 1264:56

Korup O, Montgomery DR, Hewitt K (2010) Glacier and landslide feedbacks to topographic relief in the Himalayan syntaxes. Proc Natl Acad Sci USA 107(12):5317–5322

Lee KL, Duncan JM (1975) Landslide of April 25, 1974 on the Mantaro River, Peru: National Academy of Sciences. National Research Council, Washington, DC, p 72

McCalpin J (1984) Preliminary age classification of landslides for inventory mapping: Proceedings 21st Annual Engineering Geology and Soils Engineering Symposium. University Press, Moscow, pp 99–111

Miller WJ (1931) The landslides at Point Fermin, California. Sci Mon 32:464–469

Owen L (1991) Mass movement deposits in the Karakoram Mountains: their sedimentary characteristics, recognition and role in Karakoram landform evolution. Zeitschrift fur Geomorphologie N.F 35:401–424

Reneau SL (1988) Depositional and Erosional History of Hollows: application to Landslide Location and Frequency, Long-Term Erosion Rates, and Effects of Climatic change. Ph.D Dissertation in Geology, University of California Berkeley, p 328

Rodine JM (1974) Analysis of mobilization of debris flows. Ph.D Dissertation, Scholl of Earth Sciences Stanford University, p 137

Rogers JD (1980) Factors Affecting Hillslope Profile: Current Topics in Geomorphology, U. C. Berkeley, unpublished manuscript. U. C. Water Resources Center Archives Riverside CA, p 67

Rogers JD (1994) Report Accompanying Map of Landslides and Other Surficial Deposits of the City of Orinda, CA. Consultant's report for the City of Orinda Public Works Department, p 141

Rogers JD (1998) Topographic expression of deep-seated bedrock landslide complexes. Notes accompanying evaluation and mitigation of seismic hazards. University of California Extension, Los Angeles, p 13

Selby MJ (1993) Hillslope materials and processes, 2nd edn. Oxford University Press, Oxford

Sharpe CFS (1938) Landslides and related phenomina: Columbia University Press, New York, p 137

Shehzad F, Mahmood SA, Gloaguen R (2009) Drainage network and seismological analysis of active tectonics in Nanga Parbat Haramosh Massif, Pakistan. IGARSS 1:9–12

Shroder JF (1998) Slope failure and denudation in the western Himalaya. Geomorphology 26:81–106

Shroder JF, Bishop MP (1998) Mass movement in the Himalaya: New insights and research directions. Geomorphology 26:13–35

Todd H (1930) Gilgit and Hunza river floods: correspondence. Himal J 2:173–175

Varnes DJ (1958) Landslide types and processes. In: Eckel EB (ed) Landslides and engineering practice highway research board special report29. NAS-NRC Publication544, Washington, D.C, pp 20–47

Varnes DJ (1978) Slope movement types and processes. In: Schuster RL, Krizek RJ (eds) Landslides: analysis and control, National Research Council, Washington, DC, Transportation Research Board, National Academy Press, Special Report 176, 11–33

Watkins CM, Rogers JD, and Warme JE (2007) Reconstruction of composite landslides in flat-lying sedimentary strata using graphical methods. In: Schaefer VR, Schuster RL, Turner AK (eds) First North American Landslide Conference, Conference Presentations, Association of Environmental and Engineering Geologists Special Publication 23, 488–501

Zaruba Q, Mencl V (1982) Landslides and their control, 2nd edn. Elsevier Scientific Publishing Co, Amsterdam, p 324